TOWARDS A ROBUST AUTOMATED TECHNIQUE TO CONSTRUCT AORTIC FINITE ELEMENT MESHES DIRECTLY FROM MEDICAL IMAGES

Sharareh Bayat, Dan Necsulescu and Michel Labrosse
Department of Mechanical Engineering
University of Ottawa
Ottawa, Ontario, K1N6N5
Canada

ABSTRACT

Three-dimensional (3-D) medical imaging creates new opportunities for engineering analyses, whether toward basic understanding of the physiology of an organ, or for the simulation of virtual surgical procedures. Finite element models constructed from patient-specific 3-D medical images can also be used to more fully understand a patient's pathology. However, creation of such models can be labour-intensive as it typically relies on various segmentation techniques of the organ contour in 2-D cross-sections, then the reconstruction of a 3-D surface or volume, and finally the meshing of the resulting structure. In addition, image processing and mesh generation are often operator-dependent, lack robustness and may be of suboptimal quality.

The objective of this work is to use the information contained in 3-D images to deform a structured mesh approximating an organ of interest so that it matches the geometry represented in the images. For the specific case of the aorta, our proposed methodology relies on the gradient vector flow (GVF) field and a ray-tracing algorithm to detect image boundaries and locate the center of gravity of a local cross-section; it also relies on a marching method to repeat the process between two consecutive cross-sections and generate a structured FE mesh. Testing of the methodology on simplified 3-D synthetic images yielded high quality structured meshes fast with little computational effort and minimal input from the operator. Work is underway to expand the application of the proposed methodology for robust use with images of the aorta obtained from CT or MRI scanners.

INTRODUCTION

With recent improvements and generalization of three-dimensional (3-D) medical imaging many organs can now be visualized in vivo with high resolution and accuracy. This, in turn, creates opportunities for advanced engineering analyses, whether toward basic understanding of the physiology of an organ, or for the simulation of virtual surgical procedures [1].

Finite element (FE) models constructed from patient-specific 3-D medical images can also be used to more fully understand a patient's pathology. Patient-specific FE models constructed from 3-D medical images can be used to predict deformation of the brain [2], breast [3] or the heart's left ventricle [4].

An important initial step in FE analysis is mesh generation. It involves the discretization of a 2-D or 3-D domain into small elements of simple geometry, such as triangles or tetrahedra [5]. Obviously, meshing requires the acquisition of specific geometrical information about the domain to be modeled. Mesh creation can be labour-intensive as it typically relies on various segmentation techniques of the organ contour in 2-D cross-sections [6], then the reconstruction of a 3-D surface or volume, and finally the meshing of the resulting structure. Some techniques have been introduced to automate the reconstruction process [7] but most lack robustness, and important input is still required from the user. Moreover, the reconstruction of a 3-D surface or volume is arguably a waste of resources if one is only interested in finite element meshing.

While unstructured triangular (or tetrahedral) meshes can be used to mesh nearly any 3-D surface (or volume,

respectively), these meshes are not optimal in terms of computational speed due to larger in-core memory and more CPU effort [8]. Structured meshes based on quad and hexahedral elements have been shown to perform better and to be more desirable. However, robust tools are currently missing to automatically generate structured meshes from 3-D medical images with minimum user interface.

The objective of this work is to use the information contained in 3-D images to generate a structured mesh approximating an organ of interest (here, the aorta) with minimal user input. While existing techniques use different registration methods to morph the initial mesh [9], our proposed method constructs finite element nodes directly from the images and assembles these nodes into a structured mesh. This combines the image segmentation, 3-D modeling and meshing efforts into one.

METHODS

Our proposed methodology relies on the gradient vector flow (GVF) field and a ray-tracing algorithm to detect image boundaries and locate the center of gravity of a local cross-section; it also relies on a marching method to repeat the process between two consecutive cross-sections and generate a structured FE mesh.

3-D GVF field computation

Following Xu and Prince [10], the GVF field

$$\mathbf{G}(x,y,z) = [u(x,y,z), v(x,y,z), w(x,y,z)] \quad (1)$$

is introduced as an approximation of the gradient of the known 3-D image intensity f. It is defined as the minimum of the energy functional

$$E(\mathbf{G}, f) = \iiint \mu \|\nabla \mathbf{G}\|^2 + \|\nabla f\|^2 \|\mathbf{G} - \nabla f\|^2 \, dxdydz \quad (2)$$

where ∇f is the gradient of function f. Tunable parameter μ governs the trade-off between the first and second terms in the energy functional (2). The GVF field features a large capture range and vectors that point into boundary concavities [11]. Interestingly, the GVF vectors typically change directions at the inner and/or outer layer of the boundary of an organ, depending on the imaging modality used.

Initialization

The user needs to eyeball the center of one aortic cross-section in the image volume. This cross-section is outfitted with a local Cartesian coordinate system, with x and y in the plane of the cross-section, and z perpendicular to it.

Ray-tracing algorithm (Fig. 1)

In aortic cross-section k at iteration i, the approximate center $P_k^{(i)}$ and associated coordinate system $(x_k^{(i)}, y_k^{(i)}, z_k^{(i)})$ are used to create equally spaced nodes around a small circle inside the aorta. For each of these nodes, the radius is then increased until the dot product of a local GVF vector and the local radius vector becomes negative, indicating that the node has reached the aortic wall. Thereafter, the node locations are smoothed using a central moving average method and center of gravity $P_k^{(i)}$ is determined. Convergence of the iterations for cross-section k is reached when $P_k^{(i+1)}$ and $P_k^{(i)}$ become the same point P_k, within a set precision.

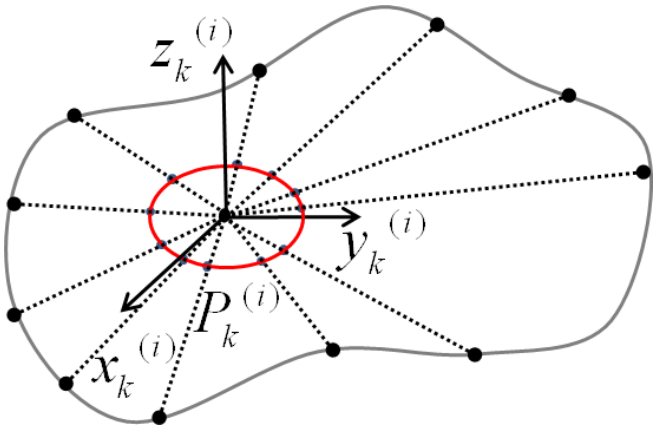

Figure 1: Partial illustration of the ray-tracing algorithm for cross-section k at iteration i. The GVF field is not represented for clarity.

Marching algorithm (Fig. 2)

From finalized cross-section k, the location and orientation of a tentative cross-section $k+1$ are created by moving P_k by some arbitrary distance along z_k, thereby defining $P_{k+1}^{(1)}$ and associated coordinate system $(x_{k+1}^{(1)}, y_{k+1}^{(1)}, z_{k+1}^{(1)})$ at iteration 1. The ray-tracing algorithm above is then used to determine a more accurate center of gravity $P_{k+1}^{(2)}$ for cross-section $k+1$. The local coordinate system is updated to $(x_{k+1}^{(1)}, y_{k+1}^{(1)}, z_{k+1}^{(1)})$ where $z_{k+1}^{(2)}$ is along $P_k P_{k+1}^{(2)}$ and appropriate rotation angles are identified to determine $x_{k+1}^{(2)}$ and $y_{k+1}^{(2)}$. Convergence of the iterations for cross-section $k+1$ is reached when $P_{k+1}^{(i+1)}$ and $P_{k+1}^{(i)}$ become the same point P_{k+1}, within a set precision.

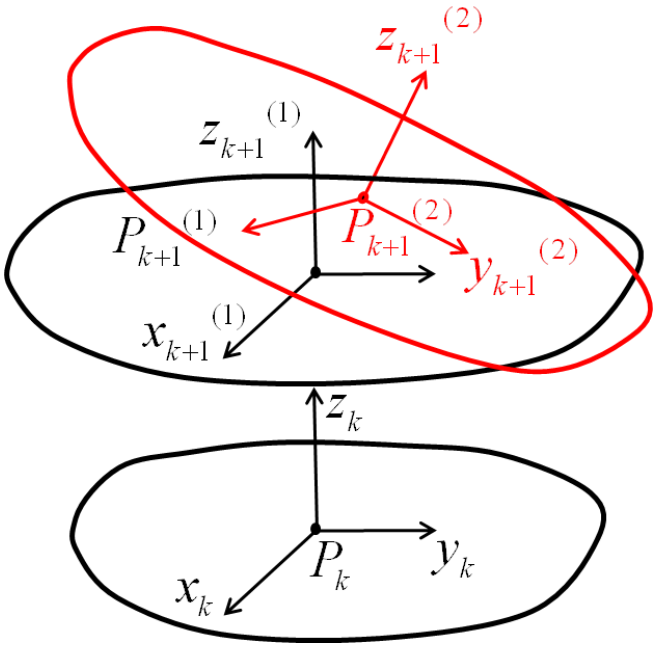

Figure 2: Partial illustration of the marching algorithm to image and mesh cross-section $k+1$ starting from cross-section k. The GVF field is not represented for clarity.

RESULTS

The proposed methodology was tested in MatLab on synthetic images representing a

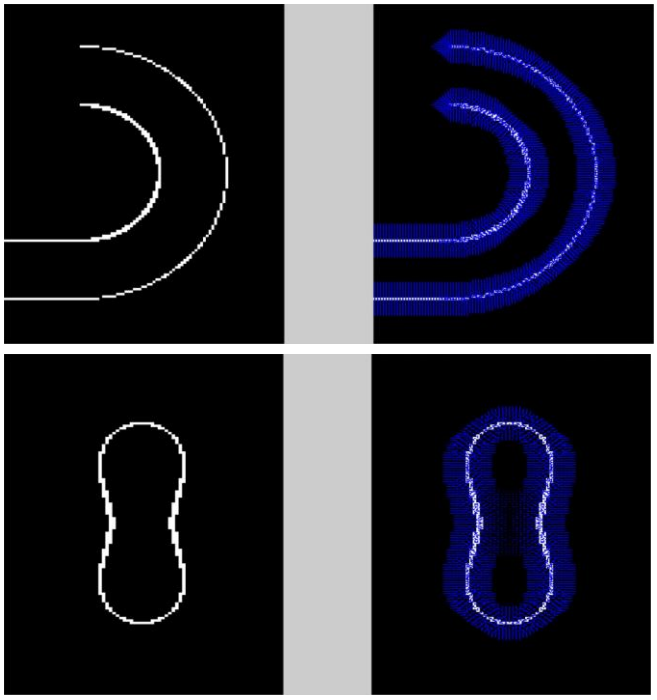

Figure 3: Implementation of 3-D GVF in synthetic images. Left: different cross-sections of the synthetic images; Right: GVF field overlaid on top of the original images.

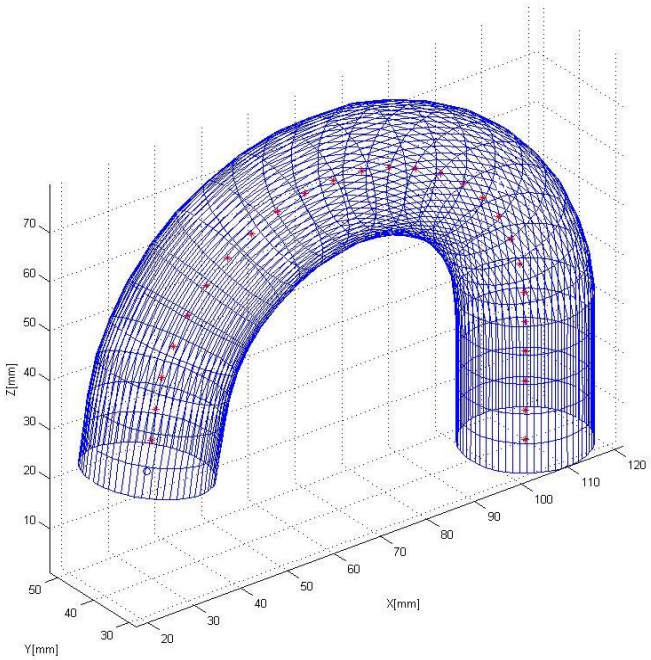

Figure 4: Structured finite element mesh of synthetic simplified human aorta. The red crosses are the centerlines detected in each cross-section. The mesh matches the dimensions of the synthetic shape.

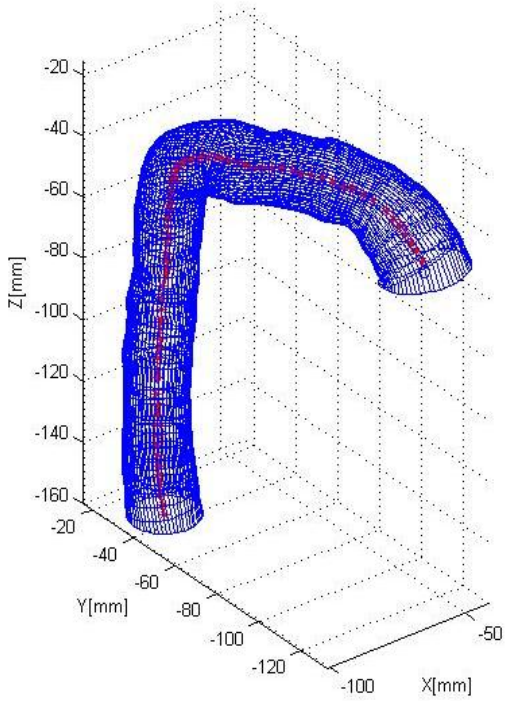

Figure 5: Resulting structured finite element mesh from proposed methodology applied to images from the Visible Human Project. The red crosses are the centerlines detected in each cross-section.

noiseless, simplified human aorta (Figs. 3, 4) as well as on a dataset available from the Visible Human Project (Fig. 5) [12].

Discussion

The proposed methodology produced high quality structured meshes with little computational effort and minimal input from the operator when noiseless synthetic images were used. Further work is underway to improve the robustness of the method in the case of real CT or MR images which usually present with significant levels of noise and complex geometries. Eventually, the methodology will have to be extended to handle branching of the main trunk of the aorta, as well as possible thrombi present in the aortic lumen.

The advantages of the proposed method are fast computational times and minimal user input. The main computational overhead is for the 3-D GVF field calculation which varies according to the density of the original dataset. It typically takes only on the order of a few minutes on any recent PC. The other sections of the algorithm take few seconds per reconstructed cross-section. Therefore, the same GVF field can be used to generate coarse or fine meshes with little difference in computational cost.

REFERENCES

[1] G. De Santis, M. De Beule, K. Canneyt, P. Segers, P. Verdonck and B. Verhegghe, "Full-hexahedral structured meshing for image-based computational vascular modeling", *Medical Engineering & Physics*, vol. 33, pp. 1318-1325, 2011.

[2] M. Ferrant, A. Nabavi, B. Macq, F. Jolesz, R. Kikinis and S. Warfield, "Registration of 3-D intraoperative MR images of the brain using a finite-element biomechanical model", IEEE Transactions *on Medical Imaging*, vol. 20, pp. 1384–1397, 2011.

[3] F. Azar, D. Metaxas and D. Schnall, "Methods for modeling and predicting mechanical deformations of the breast under external perturbations", *Medical Image Analysis*, vol. 6, no. 1, pp. 1–27, 2002.

[4] X. Papademetris, A. Sinusas, D. Dione and J. Duncan, "Estimation of 3D left ventricular deformation from echocardiography", *Medical Image Analysis*, vol. 5, no. 1, pp. 17–28, 2001.

[5] A. Mohamed and C. Davatzikos, "Finite element mesh generation and remeshing form segmented medical images", *IEEE*, pp. 7803-8388, 2004.

[6] T. Hopp et al., "Automatic multimodal 2D / 3D breast image registration using biomechanical FEM models and intensity based optimization, submitted to J. *Medical Image Analysis*, 2012.

[7] I. Sigal, M. Hardisty and C. Whyne, "Mesh-morphing algorithms for specimen-specific finite element modeling", *Journal of Biomechanics*, vol. 41, pp. 1381–1389, 2008.

[8] G. Bono and A. Awruch, "Numerical study between structured and unstructured meshes for Euler and Navier-Stokes equations", *Mecánica Computacional*, vol. XXVI. no. 36, pp.3134-3146, 2007.

[9] N. Grosland, R. Bafna and V. Magnotta, "Automated hexahedral meshing of anatomic structures using deformable registration". *Computer Methods in Biomechanics and Biomedical Engineering*, vol. 12, no. 1, pp. 35–43, 2009.

[10] C. Xu and J. Prince, "Gradient vector flow: A new external force for snakes", *IEEE Proc. Conf. on Comput. Vis. Patt. Recog. (CVPR)*, pp 66-71, 1997.

[11] L. He et al. "A comparative study of deformable contour methods on medical image segmentation", *Image and vision computing*, vol. 26, no.2, pp. 141-163, 2008.

[12] Visible Human Data Set (Male) from the National Library of Medicine, National Institutes of Health, Bethesda, vhnet.nlm.nig.gov.